Anisotropic dynamics of a spin-orbit-coupled Bose-Einstein condensate

Giovanni I. Martone,[1] Yun Li,[1] Lev P. Pitaevskii,[1,2] and Sandro Stringari[1]

[1]*Dipartimento di Fisica, Università di Trento and INO-CNR BEC Center, I-38123 Povo, Italy*

[2]*Kapitza Institute for Physical Problems, RAS, Kosygina 2, 119334 Moscow, Russia*

By calculating the density response function we identify the excitation spectrum of a Bose-Einstein condensate with equal Rashba and Dresselhaus spin-orbit coupling. We find that the velocity of sound along the direction of spin-orbit coupling is deeply quenched and vanishes when one approaches the second-order phase transition between the plane-wave and the zero momentum quantum phases. We also point out the emergence of a roton minimum in the excitation spectrum for small values of the Raman coupling, providing the onset of the transition to the stripe phase. Our findings point out the occurrence of a strong anisotropy in the dynamic behavior of the gas. A hydrodynamic description accounting for the collective oscillations in both uniform and harmonically trapped gases is also derived.

I. INTRODUCTION

Synthetic gauge fields are a developing field of research in atomic physics. They have been the object of recent experimental [1–6] and theoretical works [7–15], giving rise to the occurrence of new quantum phases exhibiting unique magnetic features, including spin-orbit-coupled configurations. The elementary excitations of such systems are also expected to exhibit novel properties [16–21]. Some of these features have already been the object of experimental measurements [5]. In particular the experiment of [5] has shown that the center-of-mass oscillation of a harmonically trapped Bose-Einstein condensate (BEC) can be deeply affected by the coupling with the spin degree of freedom, in agreement with the predictions of theory [20].

The purpose of the present work is to study the elementary excitations and the corresponding behavior of the dynamic structure factor of a spin-orbit-coupled BEC at zero temperature by direct investigation of the response of the gas to a time-dependent perturbation. We explore both the phonon regime of long wavelengths and the region at higher momentum transfer, where the spectrum exhibits features that include the occurrence of a roton minimum. Our results point out the occurrence of a strong anisotropy in the dynamic behavior of the gas. In ultracold gases the excitation spectrum can be measured via two-photon Bragg spectroscopy [22], so our predictions can be relevant for future experiments on spin-orbit-coupled BECs.

II. THE HAMILTONIAN AND THE QUANTUM PHASES

We consider a spin-1/2 Bose gas of N particles enclosed in a volume V, characterized by the single-particle Hamiltonian (we set $\hbar = m = 1$)

$$
\begin{aligned}
h_0 = {} & \frac{\mathbf{p}^2}{2} + \frac{\Omega}{2}\sigma_x \cos(2k_0 x - \Delta\omega_L t) \\
& + \frac{\Omega}{2}\sigma_y \sin(2k_0 x - \Delta\omega_L t) - \frac{\omega_Z}{2}\sigma_z,
\end{aligned} \tag{1}
$$

accounting for the presence of two laser fields with frequencies ω_L and $\omega_L + \Delta\omega_L$, wave vector difference $\mathbf{k}_0 = k_0\hat{\mathbf{e}}_x$ along the x direction, and orthogonal linear polarizations providing

transitions between the two spin states via the Raman coupling Ω. ω_Z is the Zeeman shift between the two spin states in the absence of Raman coupling [2], while σ_k, with $k = x, y, z$, are the usual 2×2 Pauli matrices. The Hamiltonian (1) is not translationally invariant but exhibits a screwlike symmetry, being invariant with respect to helicoidal translations of the form $e^{id(p_x - k_0\sigma_z)}$, consisting of a combination of a rigid translation by distance d and a spin rotation by angle $-dk_0$ around the z axis.

Let us now apply the unitary transformation $e^{i\Theta\sigma_z/2}$, corresponding to a position and time-dependent rotation in spin space by the angle $\Theta = 2k_0 x - \Delta\omega_L t$, to the wave function obeying the Schrödinger equation. As a consequence of the transformation, the single-particle Hamiltonian (1) is transformed into the translationally invariant and time-independent form

$$
h_0^{\text{SO}} = \frac{1}{2}[(p_x - k_0\sigma_z)^2 + p_\perp^2] + \frac{\Omega}{2}\sigma_x + \frac{\delta}{2}\sigma_z. \tag{2}
$$

The spin-orbit nature acquired by the Hamiltonian results from the noncommutation of the kinetic energy and the position-dependent rotation, while the renormalization of the effective magnetic field $\delta = \Delta\omega_L - \omega_Z$ results from the additional time dependence exhibited by the wave function in the rotating frame. The new Hamiltonian is characterized by equal contributions of Rashba [23] and Dresselhaus [24] couplings. It is worth pointing out that the operator $\mathbf{p}$ entering (2) is the canonical momentum $-i\nabla$, with the physical velocity being given by $\mathbf{v}_\pm = \mathbf{p} \mp k_0\hat{\mathbf{e}}_x$ for the spin-up and spin-down particles. In terms of $\mathbf{p}$ the eigenvalues of (2) are given by (we set here $\delta = 0$)

$$
\epsilon_\pm(\mathbf{p}) = \frac{p_x^2 + p_\perp^2 + k_0^2}{2} \pm \sqrt{k_0^2 p_x^2 + \frac{\Omega^2}{4}} \tag{3}
$$

and are characterized by a double-band structure.

In the presence of two-body interactions the Hamiltonian of the N-body system is given by

$$
H = \sum_j h_0^{\text{SO}}(j) + \sum_{\alpha,\beta} \frac{1}{2}\int d^3\mathbf{r}\, g_{\alpha\beta}\, n_\alpha(\mathbf{r})n_\beta(\mathbf{r}), \tag{4}
$$

where h_0^{SO} is given by (2) and α, β are the spin indices ($\uparrow, \downarrow = \pm$) characterizing the two spin states. The spin-up and spin-down density operators entering Eq. (4) are defined by $n_\pm(\mathbf{r}) = (1/2) \sum_j (1 \pm \sigma_{z,j}) \delta(\mathbf{r} - \mathbf{r}_j)$, while $g_{\alpha\beta} = 4\pi a_{\alpha\beta}$ are the relevant coupling constants in the different spin channels, with $a_{\alpha\beta}$ being the corresponding s-wave scattering lengths. Notice that the two-body interaction terms are not affected by the spin rotation discussed before.

Hamiltonian (4) has already been implemented experimentally [2,5] and has recently been employed to predict a variety of nontrivial quantum phases in Bose-Einstein condensates [11,12]. It has the peculiar property of violating both parity and time-reversal symmetry. In the presence of a spin-symmetric interaction ($g_{\uparrow\uparrow} = g_{\downarrow\downarrow} = g$ and $\delta = 0$), the quantum phases predicted by mean-field theory depend on the value of the relevant parameters k_0, Ω, and the interaction parameters [25]

$$G_1 = n(g + g_{\uparrow\downarrow})/4, \quad G_2 = n(g - g_{\uparrow\downarrow})/4, \quad (5)$$

where $n = N/V$ is the average density. In uniform matter one can use the ansatz

$$\psi = \sqrt{n} \left[C_+ \begin{pmatrix} \cos\theta \\ -\sin\theta \end{pmatrix} e^{ik_1 x} + C_- \begin{pmatrix} \sin\theta \\ -\cos\theta \end{pmatrix} e^{-ik_1 x} \right] \quad (6)$$

for the ground-state wave function of the condensate, with $|C_+|^2 + |C_-|^2 = 1$ and k_1 representing the momentum where Bose-Einstein condensation takes place. Energy minimization with respect to k_1 yields the general relationship $\theta = \arccos(k_1/k_0)/2$ fixed by the single-particle Hamiltonian (2). Minimization with respect to the other parameters eventually permits us to calculate key physical quantities such as the momentum distribution and the longitudinal ($\langle\sigma_z\rangle$) and transverse ($\langle\sigma_x\rangle, \langle\sigma_y\rangle$) spin polarization of the gas [26]:

$$\langle\sigma_z\rangle = (|C_+|^2 - |C_-|^2)\frac{k_1}{k_0}, \quad (7)$$

$$\langle\sigma_x\rangle = -\left[\frac{\sqrt{k_0^2 - k_1^2}}{k_0} + 2|C_+C_-| \cos(2k_1 x + \phi) \right], \quad (8)$$

$$\langle\sigma_y\rangle = |C_+C_-| \frac{2k_1}{k_0} \sin(2k_1 x + \phi), \quad (9)$$

where $\langle \, \rangle$ corresponds to the average in spin space divided by the average density n and ϕ is the relative phase between C_+ and C_-. The resulting ground state for $G_1 > 0$ is compatible with the three distinct BEC phases (see Fig. 1).

Phase I. For small values of the Raman coupling Ω and positive values of G_2, the ground state corresponds to a linear combination of the two plane waves $e^{\pm ik_1 x}$ with equal weight ($|C_+| = |C_-| = 1/\sqrt{2}$). This phase (hereafter called stripe phase or phase I) shares important analogies with supersolids, being characterized by the coexistence of BEC and by density modulations in the form of stripes, whose actual spatial location is the result of a mechanism of spontaneous breaking of translational invariance. The density modulations take the form $n(\mathbf{r}) = n[1 + \sqrt{1 - (k_1/k_0)^2} \cos(2k_1 x + \phi)]$, with $k_1 = k_0\sqrt{1 - \Omega^2/[2(k_0^2 + G_1)]^2}$. It is worth mentioning that these modulations differ from those of the laser potential [see Eq. (1)] and have a different nature with respect to the modulations exhibited by the density in the presence of the usual optical lattices. The contrast in $n(\mathbf{r})$ vanishes as $\Omega \to 0$
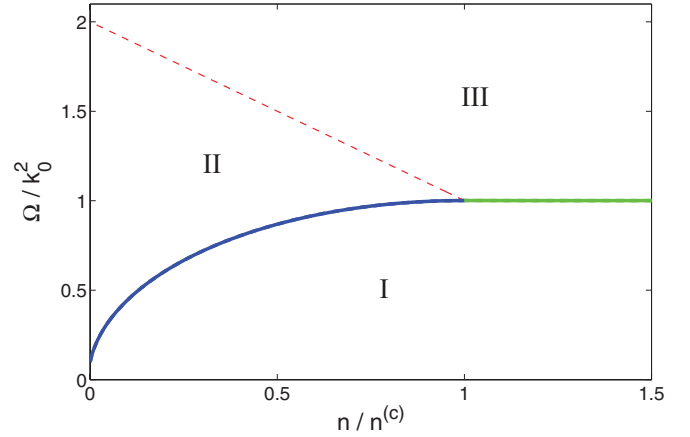

FIG. 1. (Color online) Phase diagram corresponding to the spin-orbit-coupled Hamiltonian (4). The lines corresponding to the I-II [solid blue (dark gray)], II-III (dashed red) and I-III [solid green (light gray)] phase transitions are shown. The parameters are $g = 4\pi \times 100 \, a_B$, where a_B is the Bohr radius, $\gamma = 0.0012$, and $k_0^2 = 2\pi \times 80$ Hz, corresponding to a critical density $n^{(c)} = k_0^2/(2\gamma g) = 4.37 \times 10^{15}$ cm^{-3}.

as a consequence of the orthogonality of the two spin states (in fact in this limit $\theta = 0$ and $k_1 = k_0$). In the stripe phase the longitudinal spin density identically vanishes: $\langle\sigma_z\rangle = 0$, while $\langle\sigma_x\rangle \neq 0$. It is worth mentioning that the ansatz, Eq. (6), for the stripe phase provides only a first approximation which ignores higher-order harmonics caused by the nonlinear interaction terms in the Hamiltonian.

Phase II. For larger values of the Raman coupling the system enters a new phase, the so-called plane-wave phase (hereafter called phase II), where BEC takes place in a single plane-wave state with momentum $\mathbf{p} = k_1\hat{\mathbf{e}}_x$, lying on the x axis (in the following we choose $k_1 > 0$). In this phase, the density is uniform. The spin polarization characterizing this phase is given by the simple expression $\langle\sigma_z\rangle = k_1/k_0$, with $k_1 = k_0\sqrt{1 - \Omega^2/[2(k_0^2 - 2G_2)]^2}$, while the transverse polarization is given by $\langle\sigma_x\rangle = -\Omega/[2(k_0^2 - 2G_2)]$. An energetically equivalent configuration is obtained by considering the BEC in the single-particle state with $\mathbf{p} = -k_1\hat{\mathbf{e}}_x$, the choice between the two configurations being determined by a mechanism of spontaneous symmetry breaking, typical of a ferromagnetic configuration.

Phase III. At even larger values of Ω the system enters the so-called zero momentum phase (phase III), where the condensate has zero momentum ($k_1 = 0$), the density is uniform, and the longitudinal spin polarization $\langle\sigma_z\rangle$ identically vanishes, while $\langle\sigma_x\rangle = -1$.

The chemical potential in the three phases can be calculated following the procedure of [12] and is given by

$$\mu^{(I)} = 2G_1 - \frac{k_0^2 \Omega^2}{8\left(k_0^2 + G_1\right)^2}, \quad (10)$$

$$\mu^{(II)} = 2\left(G_1 + G_2\right) - \frac{k_0^2 \Omega^2}{8\left(k_0^2 - 2G_2\right)^2}, \quad (11)$$

$$\mu^{(III)} = 2G_1 + \frac{k_0^2 - \Omega}{2}. \quad (12)$$

The critical values of the Raman frequencies Ω characterizing the phase transitions are obtained by imposing that the chemical potential and the pressure $P = n\mu(n) - \int \mu(n)dn$ be equal in the two phases at equilibrium. One finds that the transition between phases I and II has a first-order nature and is characterized by different values of the densities of the two phases. The density differences are, however, extremely small and are not visible in Fig. 1. The transition between phases II and III has instead a second-order nature and is characterized by a jump in the compressibility $n^{-1}(\partial\mu/\partial n)^{-1}$ if $G_2 \neq 0$ and by a divergent behavior of the spin polarizability (see Sec. IV). For small values of the coupling constants $(G_1, G_2 \ll k_0^2)$ the critical value of the Raman coupling $\Omega^{(\text{I-II})}$ between phases I and II is given by the density-independent expression [11,12]

$$\Omega^{(\text{I-II})} = 2k_0^2\sqrt{\frac{2\gamma}{1+2\gamma}}, \tag{13}$$

with $\gamma = G_2/G_1$. The transition between phases II and III instead takes place at the higher value [12]

$$\Omega^{(\text{II-III})} = 2(k_0^2 - 2G_2), \tag{14}$$

provided that the condition $k_0^2 > 4G_2(1 + \gamma)$ is satisfied; in the opposite case one instead has the first-order transition directly between phases I and III [12]. One should finally recall that if $G_2 < 0$ only phases II and III are available, with the stripe phase being always energetically unfavorable.

III. DENSITY RESPONSE FUNCTION

In order to calculate the dynamic density response of the system we add the time-dependent perturbation $V_\lambda = -\lambda e^{i(\mathbf{q}\cdot\mathbf{r}-\omega t)} + \text{H.c.}$ to the single-particle Hamiltonian (2). The direction of the wave vector $\mathbf{q}$ is characterized by the polar angle $0 \leqslant \alpha \leqslant \pi$ with respect to the x axis. The density response function is then calculated through the usual definition $\chi(\mathbf{q},\omega) = \lim_{\lambda \to 0} \delta\rho_{\mathbf{q}}/(\lambda e^{-i\omega t})$, where $\delta\rho_{\mathbf{q}}$ are the fluctuations of the $\mathbf{q}$ component of the density induced by the external perturbation. In the following we calculate $\chi(\mathbf{q},\omega)$ by solving the time-dependent Gross-Pitaevskii equation

$$i\partial_t\psi = \left[h_0^{\text{SO}} + V_\lambda + \frac{2G_1}{n}(\psi^\dagger\psi) + \frac{2G_2}{n}(\psi^\dagger\sigma_z\psi)\sigma_z\right]\psi, \tag{15}$$

where h_0^{SO} is the single-particle Hamiltonian (2) with $\delta = 0$. We restrict the analysis to phases II and III, where the ground-state density is uniform and the wave function of the condensate can be written in the simple form

$$\psi = \sqrt{n}\left[\begin{pmatrix}\cos\theta \\ -\sin\theta\end{pmatrix}e^{ik_1x} + \begin{pmatrix}u_\uparrow(\mathbf{r}) \\ u_\downarrow(\mathbf{r})\end{pmatrix}e^{-i\omega t}\right.$$
$$\left. + \begin{pmatrix}v_\uparrow^*(\mathbf{r}) \\ v_\downarrow^*(\mathbf{r})\end{pmatrix}e^{i\omega t}\right]e^{-i\mu t}. \tag{16}$$

The terms depending on the Bogoliubov amplitudes u and v provide the deviations in the order parameter with respect to equilibrium, caused by the external perturbation. In the linear, small λ limit we find the result (near the poles one should replace ω with $\omega + i0$)

$$\chi(\mathbf{q},\omega) = \frac{-Nq^2[\omega^2 - 4k_1q\cos\alpha\,\omega + a(q,\alpha)]}{\omega^4 - 4k_1q\cos\alpha\,\omega^3 + b_2(q,\alpha)\omega^2 + k_1q\cos\alpha\,b_1(q,\alpha)\omega + b_0(q,\alpha)}, \tag{17}$$

where the coefficients a and b_i are even functions of $q \equiv |\mathbf{q}|$ and $\cos\alpha$, implying that $b_i(q,\alpha) = b_i(q,\pi \pm \alpha)$ and $a(q,\alpha) = a(q,\pi \pm \alpha)$, and their actual values depend on whether one is in phase II or III (see the Appendix).

The above equations include all the relevant information relative to the frequency of the elementary excitations, given by the poles of χ, i.e., by the zeros of

$$\omega^4 - 4k_1q\cos\alpha\,\omega^3 + b_2\omega^2 + k_1q\cos\alpha\,b_1\omega + b_0 = 0, \tag{18}$$

as well as to the dynamic structure factor given, at $T = 0$, by

$$S(\mathbf{q},\omega) = \pi^{-1}\text{Im}\chi(\mathbf{q},\omega) \tag{19}$$

for $\omega \geqslant 0$ and $S(\mathbf{q},\omega) = 0$ for negative ω. In particular the f-sum rule $\int d\omega S(\mathbf{q},\omega)\omega = Nq^2/2$ is exactly satisfied, as one can deduce from the correct large ω behavior of the density response function: $\chi(\mathbf{q},\omega)_{\omega\to\infty} = -Nq^2/\omega^2$ [27]. It is also worth pointing out that the density response function is invariant with respect to the unitary transformation yielding the Hamiltonian in the spin-rotated frame, so that the results presented in this paper, based on Eq. (17),

hold also in the original frame and are relevant for actual experiments.

Equation (17) reduces to a simplified form in two limiting cases. A first case is when $G_2 = 0$ and $\Omega = 0$. In this limit the denominator can be rewritten in a factorized form, and χ reduces to the usual Bogoliubov form $\chi(\mathbf{q},\omega) = -Nq^2/[\omega^2 - q^2(2G_1 + q^2/4)]$, characterizing the response of a BEC gas in the absence of spin-orbit coupling. A second case is the ideal Bose gas $(G_1 = G_2 = 0)$, where H reduces to the single-particle Hamiltonian (2) with $\delta = 0$ and the excitation spectrum, given by the solutions of Eq. (18), takes the simple form

$$\omega_\pm(\mathbf{q}) = \epsilon_\pm(\mathbf{p}_1 + \mathbf{q}) - \epsilon_-(\mathbf{p}_1), \tag{20}$$

where $\mathbf{p}_1 = k_1\hat{\mathbf{e}}_x$ is the momentum where Bose-Einstein condensation takes place and $\epsilon_\pm$ are the two branches of the single-particle spectrum (3).

It is worth noticing that the odd terms in ω entering the response function identically vanish in the zero momentum phase III but survive in phase II, reflecting the lack of parity and time-reversal symmetry of the ground-state wave function.

The condition $\text{Im}\chi(\mathbf{q}, \omega) = -\text{Im}\chi(-\mathbf{q}, -\omega)$, characterizing the imaginary part of the response function, is always satisfied, but the symmetry relationship $\text{Im}\chi(\mathbf{q}, \omega) = \text{Im}\chi(-\mathbf{q}, \omega)$ is not ensured in phase II, where one consequently finds $S(\mathbf{q}, \omega) \neq S(-\mathbf{q}, \omega)$. The first results for the excitation spectrum of Hamiltonian (4) for small and large values of Ω, far from the transition between the plane-wave and the zero momentum phases, have recently been discussed in [21] using a hydrodynamic formalism.

Equation (17) permits us to calculate the static response function $\chi(\mathbf{q}) \equiv \chi(\mathbf{q}, \omega = 0)/N$, yielding the results

$$\mathcal{K}_{\text{II}}^{-1} = 2G_1 + \frac{2G_2 k_1^2 \left(k_1^2 \cos^2\alpha + k_0^2 \sin^2\alpha - 2G_2\right)}{k_1^2 \left(k_0^2 \cos^2\alpha - 2G_2\right) + k_0^4 \sin^2\alpha}, \quad (21)$$

$$\mathcal{K}_{\text{III}}^{-1} = 2G_1 \quad (22)$$

for the $q = 0$ value $\mathcal{K} \equiv \chi(q = 0)$ of the static response in phases II and III, respectively. Result (21) depends on the polar angle α, revealing the anisotropy of $\mathcal{K}$ in the plane-wave phase caused by the spin-interaction term G_2. It is also worth pointing out that, if $\cos\alpha \neq \pm 1$, in phase II the $q = 0$ static response $\mathcal{K}$ differs from the thermodynamic compressibility $n^{-1}(\partial\mu/\partial n)^{-1}$, with μ calculated from (11). Furthermore, if $\cos\alpha = \pm 1$ and $G_2 \neq 0$, the $q = 0$ static response $\mathcal{K}$ exhibits a jump at the transition between phases II and

III. One can easily prove that the frequencies $\omega(\mathbf{q})$ of the elementary excitations, given by the zeros of (18), are instead always continuous functions of the Raman coupling Ω at the transition for all values of $\mathbf{q}$.

IV. VELOCITY OF SOUND AND THE ROLE OF THE MAGNETIC SUSCEPTIBILITY

The low-frequency excitations at small q (sound waves) can be easily obtained by setting $\omega = cq$ and keeping the leading terms in q^2 in (18). In phase III we find the result

$$c_{\text{III}} = \sqrt{2G_1 \left(1 - \frac{2k_0^2 \cos^2\alpha}{\Omega + 4G_2}\right)}, \quad (23)$$

which explicitly shows the strong reduction of the sound velocity along the x direction ($\cos\alpha = \pm 1$) caused by the spin-orbit coupling when one approaches the transition to the plane-wave phase. The quenching can be understood in terms of the increase of the effective mass associated with the single-particle spectrum (3). At the transition, where the velocity of sound propagating along the x direction vanishes, the elementary excitations exhibit a different q^2 dependence. On the other hand, the sound velocities along the other directions ($\alpha \neq 0$ and π) remain finite at the transition. In the plane-wave phase, phase II, the sound velocity is instead given by

$$c_{\text{II}} = \frac{\sqrt{2\left[G_1 k_0^4 + G_2 k_1^2 (k_0^2 - 2G_1 - 2G_2)\right]\left[k_0^4 - 2G_2 k_1^2 - k_0^2(k_0^2 - k_1^2)\cos^2\alpha\right]} + 2G_2 k_1 (k_0^2 - k_1^2)\cos\alpha}{k_0^4 - 2G_2 k_1^2} \quad (24)$$

and exhibits a further interesting feature caused by the lack of parity symmetry. The asymmetry effect in the sound velocity is due to the presence of the last term in the numerator of Eq. (24); therefore the symmetry will be recovered if $G_2 = 0$ or $\alpha = \pi/2$ (corresponding to phonons propagating along the directions orthogonal to the x axis). Also in phase II, the velocity of sound along the x direction vanishes when one approaches the transition to phase III.

In order to better understand the role played by the spin degree of freedom in the propagation of sound, it is interesting to relate the sound velocity to the magnetic polarizability, which can be calculated by generalizing the ground-state condensate wave function (6) in the presence of a static magnetic field h coupled to the system through the interaction term $-h\sigma_z$. To calculate the new ground state we replace the variational parameters θ and k_1 entering the ansatz (6) with two independent sets of parameters, θ_+, k_1^+ and θ_-, k_1^-, characterizing the two plane waves, and we minimize the energy. In the small h limit the magnetic polarizability is determined by $\mathcal{M} = \int d^3r\langle\sigma_z\rangle/(hV)$. After some straightforward algebra we find the following results hold, respectively, in phases II and III [20]:

$$\mathcal{M}_{\text{II}} = \frac{k_0^2 - k_1^2}{k_1^2 \left(k_0^2 - 2G_2\right)}, \quad (25)$$

$$\mathcal{M}_{\text{III}} = \frac{2}{\Omega - 2\left(k_0^2 - 2G_2\right)}. \quad (26)$$

A peculiar feature exhibited by the above equations is the divergent behavior near the second-order phase transition II-III where $\Omega = 2(k_0^2 - 2G_2)$ and $k_1 = 0$. In terms of the $q = 0$ static response $\mathcal{K}$ and the magnetic susceptibility $\mathcal{M}$ one can rewrite the results for the sound velocity in the useful form

$$c(\alpha)c(\alpha + \pi) = \frac{1 + k_0^2 \mathcal{M} \sin^2\alpha}{\mathcal{K}\left(1 + k_0^2 \mathcal{M}\right)}, \quad (27)$$

which holds in both phases II and III. Equation (27) generalizes the usual relation $c^2 = n(\partial\mu/\partial n)$ between the sound velocity and the compressibility holding in the usual superfluids. It explicitly shows that, along the x direction, where $\sin\alpha = 0$, the sound velocity c vanishes at the transition because of the divergent behavior of the magnetic polarizability. The results for the sound velocity along the x axis are shown in Fig. 2 for a configuration with relatively large G_2, emphasizing the difference between $c_{\text{II}}^+(\alpha = 0)$ and $c_{\text{II}}^-(\alpha = \pi)$, i.e., between the velocities of sound waves propagating in opposite directions along the x axis. Notice that the sound velocity, in the absence of spin-orbit and Raman coupling, would correspond to the value $c = \sqrt{2G_1}$ (horizontal dashed line). This value is asymptotically reached only for very large values of Ω. The quenching effect exhibited by the sound velocity near the II-III phase transition is particularly remarkable in the zero momentum phase, phase III, where BEC takes place in the $\mathbf{p} = 0$ state and the
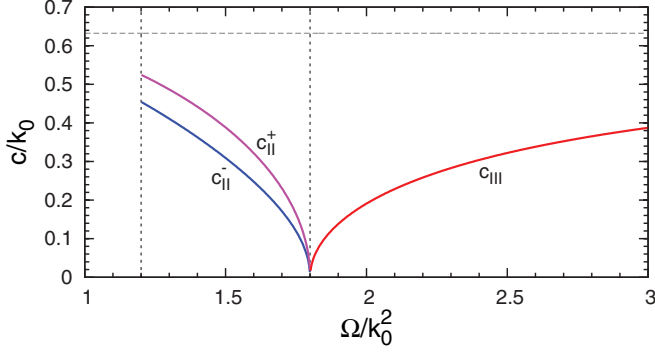
FIG. 2. (Color online) Sound velocity as a function of the Raman coupling for the following choice of parameters: $G_1/k_0^2 = 0.2$, $G_2/k_0^2 = 0.05$. The two sound velocities in phase II correspond to phonons propagating in the directions parallel ($c_{\rm II}^+$) and antiparallel ($c_{\rm II}^-$) to k_1. The horizontal dashed line corresponds to the value $\sqrt{2G_1} = 0.63\,k_0$ of the sound velocity in the absence of spin-orbit and Raman coupling. The vertical dashed lines indicate the Raman frequencies at which the I-II and II-III phase transitions take place.

compressibility of the gas is unaffected by spin-orbit coupling. It explicitly reveals the mixed density and magnetic nature of the sound waves, with the spin nature becoming more and more important as one approaches the phase transition where $\mathcal{M}$ diverges.

It is finally interesting to understand the role played by the sound waves in terms of sum rules. From Eq. (17) one can easily prove that phonons exhaust the compressibility sum rule $\int_{-\infty}^{+\infty} d\omega S(\mathbf{q},\omega)/\omega$ at small q but, different from ordinary superfluids, they give only a small contribution to the f-sum rule $\int_{-\infty}^{+\infty} d\omega S(\mathbf{q},\omega)\omega = Nq^2/2$ as one approaches the transition [28]. This contribution becomes vanishingly small at the transition for wave vectors $\mathbf{q}$ oriented along the x direction. Also, the static structure factor $S(\mathbf{q}) = \int_0^\infty d\omega S(\mathbf{q},\omega)/N$ is strongly quenched compared to the usual BECs. This results in an enhancement of the quantum fluctuations of the order parameter, as predicted by the uncertainty principle inequality [29]. The effect is, however, small because the sound velocity vanishes only along the x direction [12].

V. ROTON AND MAXON EXCITATIONS

When one moves far from the phonon regime, new interesting features emerge from the study of the response function. First, the poles of Eq. (17) provide two separated branches [see Figs. 3(a) and 3(b)], with the lower one approaching the phonon dispersion at small q. For example, in phase III, where the excitation spectrum is symmetric under inversion of $\mathbf{q}$ into $-\mathbf{q}$, the gap between the two branches is given, at $\mathbf{q} = 0$, by $\Delta = \sqrt{\Omega(\Omega + 4G_2)}$.

A very peculiar feature of the lower branch is exhibited in the plane-wave phase, phase II, for negative values of q_x, resulting in the emergence of a roton minimum [21] which becomes more and more pronounced as one approaches the phase transition to the stripe phase, phase I. The occurrence of the rotonic structure in spin-orbit-coupled BEC gases
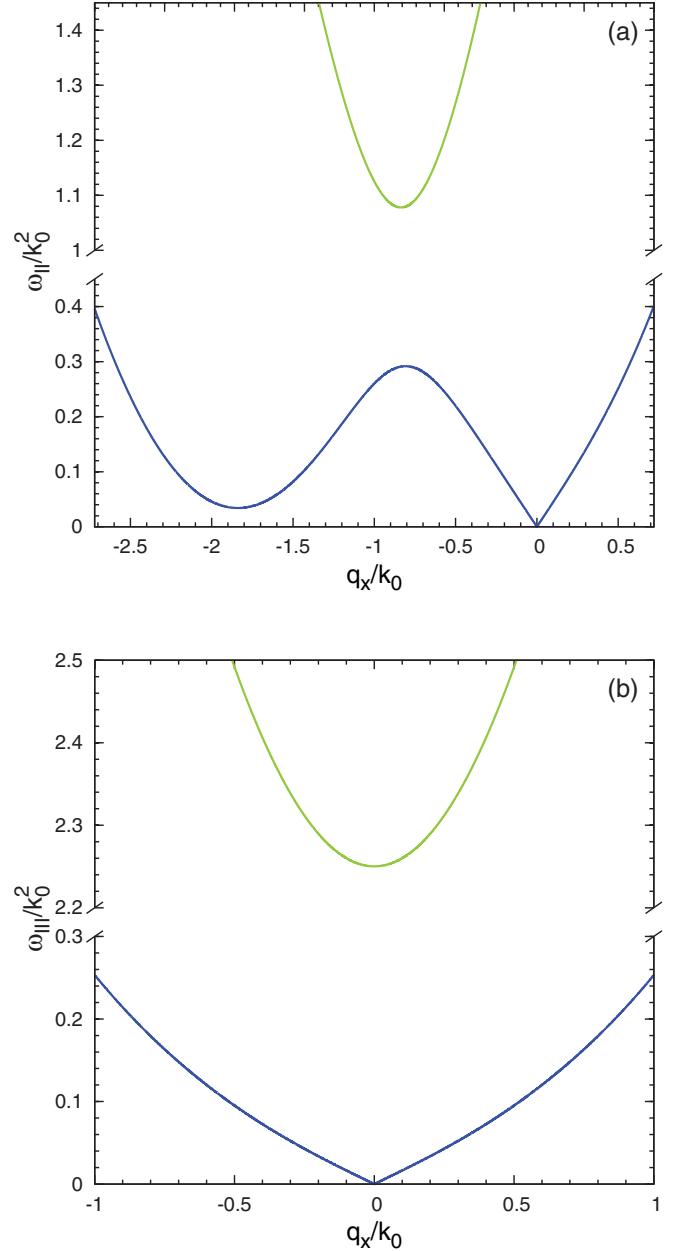

FIG. 3. (Color online) Excitation spectrum (a) in phase II ($\Omega/k_0^2 = 0.85$) and (b) in phase III ($\Omega/k_0^2 = 2.25$) as a function of q_x ($q_y = q_z = 0$). The blue (dark gray) and green (light gray) lines represent the lower and upper branches, respectively. In phase II the spectrum is not symmetric and exhibits a roton minimum for negative q_x, whose energy becomes smaller and smaller as one approaches the transition to the stripe phase at $\Omega/k_0^2 = 0.09$. The other parameters are $G_1/k_0^2 = 0.12$ and $\gamma = G_2/G_1 = 10^{-3}$.

shares interesting analogies with the case of dipolar gases in quasi-two-dimensional configurations [30]. In Fig. 3(a) we show the excitation spectrum in phase II, calculated in the experimental conditions of [5], for wave vectors $\mathbf{q}$ lying on the x axis. In Fig. 3(b) we instead show the excitation spectrum in phase III, which, different from Fig. 3(a), exhibits symmetry under inversion of q_x into $-q_x$. The physical origin of the roton minimum is quite clear. In phase II the ground state is degenerate, and it is very favorable for atoms to be transferred
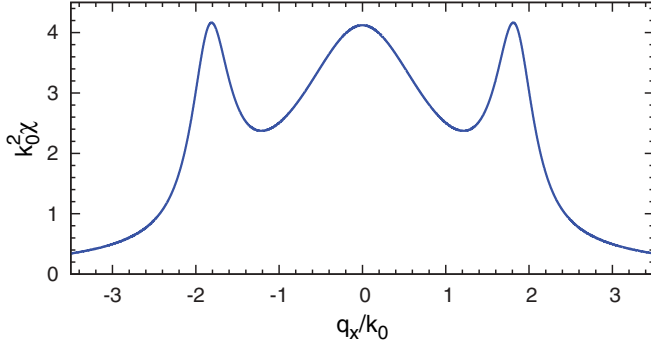
FIG. 4. (Color online) Static response in phase II as a function of q_x ($q_y = q_z = 0$). The curve is symmetric and exhibits a typical peak near the roton momentum. The parameters are $\Omega/k_0^2 = 0.85$, $G_1/k_0^2 = 0.12$, and $\gamma = G_2/G_1 = 10^{-3}$.

from the BEC state at $\mathbf{p} = \mathbf{p}_1$ to the empty state at $\mathbf{p} = -\mathbf{p}_1$. The occurrence of the roton minimum is also reflected in a strong enhancement in the static response function $\chi(q_x)$ (see Fig. 4). Notice that $\chi(q_x)$, different from $\omega(q_x)$, is always a symmetric function of q_x. The occurrence of the roton minimum in the excitation spectrum and the corresponding enhancement of the static response represent a typical tendency of the system towards crystallization. In the case of excitations propagating along the x axis we have investigated in detail the condition for the roton frequency being equal to zero, corresponding to a divergent behavior for $\chi(q_x)$. A simple analytic expression for the corresponding value of the Raman coupling Ω is obtained in the weak-coupling limit $G_1, G_2 \ll k_0^2$, where we find that the critical value exactly coincides with the value given by Eq. (13) characterizing the transition between the plane-wave and the stripe phases. For larger values of the coupling constants G_1 and G_2 we expect that the critical value takes place for values of the Raman coupling smaller than the value at the transition, exhibiting the typical spinoidal behavior of first-order liquid-crystal phase transitions.

Despite the divergent behavior exhibited by the static response function $\chi(q_x)$, the static structure factor $S(q_x)$ does not exhibit any peaked structure near the roton point, different from what happens, for example, in superfluid helium [31]. In Fig. 5 we show $S(q_x)$ together with the contribution to
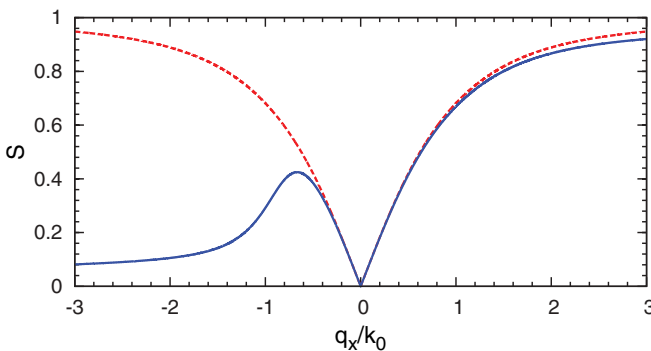

FIG. 5. (Color online) Contribution of the lower branch to the static structure factor in phase II as a function of q_x (blue solid line) compared with the total $S(q_x)$ (red dashed line). The parameters are $\Omega/k_0^2 = 0.85$, $G_1/k_0^2 = 0.12$, and $\gamma = G_2/G_1 = 10^{-3}$.

the integral $S(q_x) = \int d\omega S(q_x, \omega)/N$ arising from the lower branch of the elementary excitations. In Fig. 5 we have chosen $q_y = q_z = 0$. Figure 5 shows that the lower-branch contribution is not symmetric for exchange of q_x into $-q_x$, even if the total $S(q_x)$ is symmetric [32]. Remarkably, Fig. 5 shows that the strength carried by the lower branch is significantly peaked for intermediate values of q_x between the phonon and the roton regimes, in the so-called maxon region, where the lower-branch excitation spectrum exhibits a maximum [see Fig. 3(a)].

VI. HYDRODYNAMIC FORMALISM

The peculiar behavior of the excitation spectrum in the phonon regime discussed in Sec. IV can be usefully described using the hydrodynamic formalism where one writes the spin-up and spin-down components of the order parameter in terms of their modulus and phase [21]. In this case one finds four coupled equations instead of two equations as in usual BECs. In the phonon regime of large wavelengths and small frequencies one can safely neglect the quantum pressure terms. Furthermore, one finds that the phase difference between the two spin components is blocked ($\varphi_\uparrow = \varphi_\downarrow$). This is the consequence of the equation for the spin density and the fact that $\omega \ll \Omega$ [33]. By imposing the condition $\varphi \equiv \varphi_\uparrow = \varphi_\downarrow$, which holds for small frequencies, one then derives the nontrivial relationship

$$k_0 \nabla_x \delta\varphi - k_0^2 Z \left(-\frac{s}{n}\frac{\delta n}{n} + \frac{\delta s}{n} \right) - 2G_2 \frac{\delta s}{n} = 0 \quad (28)$$

between the phase gradient, the density, and the spin fluctuations. In the above equation $s = nk_1/k_0$ is the spin density relative to the equilibrium configuration, and we have defined the relevant parameter

$$Z = \frac{\Omega}{2k_0^2 \left(1 - k_1^2/k_0^2\right)^{3/2}}. \quad (29)$$

Equation (28) permits us to reduce the hydrodynamic equations

$$\partial_t \delta n + \boldsymbol{\nabla} \cdot (n \boldsymbol{\nabla} \delta\varphi) - k_0 \nabla_x \left[n \left(-\frac{s}{n}\frac{\delta n}{n} + \frac{\delta s}{n} \right) \right] = 0, \quad (30)$$

$$\partial_t \delta\varphi + k_1 \nabla_x \delta\varphi - k_0^2 Z \frac{s}{n} \left(-\frac{s}{n}\frac{\delta n}{n} + \frac{\delta s}{n} \right) + 2G_1 \frac{\delta n}{n} = 0 \quad (31)$$

for the density and the phase, respectively, to a closed set of coupled equations. The solutions of the hydrodynamic equations reproduce exactly results (23) and (27) for the sound velocity. It is particularly worth pointing out the crucial changes caused by the spin-orbit term in the equation of continuity [Eq. (30)]. These changes reflect the fact that the current is not simply given by the canonical momentum operator but is affected by the spin variable. The current density operator should actually satisfy the continuity equation $[H, n(\mathbf{r})] = i\boldsymbol{\nabla} \cdot \mathbf{j}(\mathbf{r})$, where $n(\mathbf{r}) = \sum_k \delta(\mathbf{r} - \mathbf{r}_k)$ is the density operator. By explicitly carrying out the commutator one identifies the current as $\mathbf{j}(\mathbf{r}) = \mathbf{p}(\mathbf{r}) - k_0 \sigma_z(\mathbf{r}) \hat{\mathbf{e}}_x$, where $\mathbf{p}(\mathbf{r}) = \sum_k [\mathbf{p}_k \delta(\mathbf{r} - \mathbf{r}_k) + \text{H.c.}]/2$ and $\sigma_z(\mathbf{r}) = \sum_k \sigma_{z,k} \delta(\mathbf{r} - \mathbf{r}_k)$ are the momentum and spin density, respectively.

The hydrodynamic equations also permit us to calculate the relative amplitudes of the density and spin-density oscillations characterizing the propagation of sound. In terms of the magnetic polarizability $\mathcal{M}$ we find

$$\left(\frac{\delta s}{\delta n}\right)_{\mathrm{II}} = \frac{k_0 \mathcal{M} \cos\alpha}{1 + k_0^2 \mathcal{M}} \sqrt{\frac{2\left[G_2 + G_1\left(1 + k_0^2 \mathcal{M}\right)\right]}{1 + k_0^2 \mathcal{M} \sin^2\alpha}}$$
$$+ \frac{\sqrt{1 + \left(k_0^2 - 2G_2\right)\mathcal{M}}}{1 + k_0^2 \mathcal{M}}, \tag{32}$$

$$\left(\frac{\delta s}{\delta n}\right)_{\mathrm{III}} = \frac{2k_0 \mathcal{M} \cos\alpha \sqrt{G_1}}{\sqrt{2\left(1 + k_0^2 \mathcal{M}\right)\left(1 + k_0^2 \mathcal{M} \sin^2\alpha\right)}} \tag{33}$$

in phases II and III, respectively. Equations (32) and (33) show that, near the transition between phases II and III, the amplitude of the spin-density fluctuations δs of the sound waves propagating along the x direction ($\sin\alpha = 0$) are strongly enhanced with respect to the density fluctuations δn as a consequence of the divergent behavior of the magnetic susceptibility. This suggests that an effective way to excite these phonon modes is through a coupling with the spin degree of freedom, as recently achieved in two-photon Bragg experiments on Fermi gases [34]. For sound waves propagating in the direction orthogonal to x the situation is instead different. In particular in phase III sound waves are purely density oscillations ($\delta s = 0$).

A major advantage of the hydrodynamic equations is that they can be easily extended to trapped nonuniform configurations. In the simplest $G_2 = 0$ case, corresponding to $G_1 = ng/2$, where the wave vector $\mathbf{p}_1 = k_1 \hat{\mathbf{e}}_x$ is density independent, the chemical potential is given by the Bogoliubov form $\mu = gn + \kappa$, with κ being independent of the density in both phases II and III, and the three-dimensional hydrodynamic equations can be reduced to the compact form

$$\partial_t^2 \delta n = g\left[(1 - 1/Z)\,\nabla_x\,(n\nabla_x\delta n) + \nabla_\perp \cdot (n\nabla_\perp\delta n)\right]. \tag{34}$$

Here n is the Thomas-Fermi density profile given, in the presence of harmonic trapping $V_{\mathrm{ho}}(\mathbf{r}) = (\omega_x^2 x^2 + \omega_y^2 y^2 + \omega_z^2 z^2)/2$, by an inverted parabola: $n(\mathbf{r}) = [\mu_0 - V_{\mathrm{ho}}(\mathbf{r})]/g$, with μ_0 fixed by the normalization condition. One can easily check that all the solutions that hold for usual BECs [35] still hold in the presence of spin-orbit coupling, with the simple replacement of the trapping frequency ω_x with $\omega_x\sqrt{1 - 1/Z}$. This reproduces the result

$$\omega_D^2 = \frac{\omega_x^2}{1 + k_0^2 \mathcal{M}} \tag{35}$$

derived in [20] for the frequency of the dipole oscillation along the x axis using a sum rule approach and also shows that the frequency of the other hydrodynamic modes involving a motion of the gas along the x axis will be quenched. The quenching of the dipole mode due to spin-orbit coupling has been recently observed in the experiment of [5].

VII. CONCLUSION

In conclusion we have investigated the dynamic behavior of a Bose-Einstein condensate with spin-orbit coupling, pointing out the occurrence of features of high relevance for future experiments, such as the strong quenching exhibited by the sound velocity near the second-order transition between the plane-wave and the zero momentum phases, the anisotropy of the compressibility, and the occurrence of a roton minimum in the excitation spectrum. Our theoretical predictions can be tested in future experiments based on two-photon Bragg spectroscopy and are expected to deeply influence the superfluid behavior of the gas.

APPENDIX: THE COEFFICIENTS IN THE RESPONSE FUNCTION

The coefficients in response function (17) can be expressed as follows. In phase II we find

$$a = -\frac{q^4}{4} + \left[\left(k_0^2 + 3k_1^2\right)\cos^2\alpha - 2\left(k_0^2 - G_2\right) + 2G_2 k_1^2/k_0^2\right]q^2$$
$$+ 4\left(k_0^2 - 2G_2\right)\left[\left(k_0^2 - k_1^2\right)\cos^2\alpha - k_0^2 + 2G_2 k_1^2/k_0^2\right],$$

$$b_0 = \frac{q^8}{16} - \left[\left(k_0^2 + k_1^2\right)\cos^2\alpha - k_0^2 - G_1 + G_2\right]\frac{q^6}{2}$$
$$+ \left\{\left(k_0^2 - k_1^2\right)^2\cos^4\alpha - 2\left[k_0^2\left(k_0^2 - k_1^2\right)\right.\right.$$
$$+ G_1\left(k_0^2 + 3k_1^2\right) - G_2\left(k_0^2 - 5k_1^2\right)\right]\cos^2\alpha$$
$$+ k_0^2\left(k_0^2 - 2G_2\right) + 4G_1\left(k_0^2 - G_2\right)$$
$$+ 2\left(k_0^2 - 2G_1 - 2G_2\right)G_2 k_1^2/k_0^2\right\}q^4$$
$$- 8\left(k_0^2 - 2G_2\right)\left[\left(k_0^2 - k_1^2\right)\left(G_1 + G_2 k_1^2/k_0^2\right)\cos^2\alpha\right.$$
$$- G_1 k_0^2 - \left(k_0^2 - 2G_1 - 2G_2\right)G_2 k_1^2/k_0^2\right]q^2,$$

$$b_1 = q^4 + 4\left[\left(k_0^2 - k_1^2\right)\cos^2\alpha + 2\left(G_1 + G_2\right)\right]q^2$$
$$+ 16\left(k_0^2 - 2G_2\right)\left(k_0^2 - k_1^2\right)G_2/k_0^2,$$

$$b_2 = -\frac{q^4}{2} - 2\left[\left(k_0^2 - 3k_1^2\right)\cos^2\alpha + k_0^2 + G_1 - G_2\right]q^2$$
$$- 4\left(k_0^2 - 2G_2\right)\left(k_0^2 - 2G_2 k_1^2/k_0^2\right).$$

In phase III we instead obtain the results

$$a = -\frac{q^4}{4} - \left(\Omega - k_0^2\cos^2\alpha + 2G_2\right)q^2$$
$$- \Omega\left[\Omega - 2\left(k_0^2\cos^2\alpha - 2G_2\right)\right],$$

$$b_0 = \frac{q^8}{16} + \left[\Omega - 2\left(k_0^2\cos^2\alpha - G_1 - G_2\right)\right]\frac{q^6}{4}$$
$$+ \left[\Omega^2 - 4\left(k_0^2\cos^2\alpha - 2G_1 - G_2\right)\Omega\right.$$
$$+ 4\left(k_0^2\cos^2\alpha - 2G_1\right)\left(k_0^2\cos^2\alpha - 2G_2\right)\right]\frac{q^4}{4}$$
$$+ 2G_1\Omega\left[\Omega - 2\left(k_0^2\cos^2\alpha - 2G_2\right)\right]q^2,$$

$$b_1 = 0,$$

$$b_2 = -\frac{q^4}{2} - \left[\Omega + 2\left(k_0^2\cos^2\alpha + G_1 + G_2\right)\right]q^2$$
$$- \Omega(\Omega + 4G_2).$$

[1] Y.-J. Lin, R. L. Compton, A. R. Perry, W. D. Phillips, J. V. Porto, and I. B. Spielman, Phys. Rev. Lett. **102**, 130401 (2009); Y.-J. Lin, R. L. Compton, K. Jiménez-García, J. V. Porto, and I. B. Spielman, Nature (London) **462**, 628 (2009); Y.-J. Lin, R. L. Compton, K. Jiménez-García, W. D. Phillips, J. V. Porto, and I. B. Spielman, Nat. Phys. **7**, 531 (2011).

[2] Y.-J. Lin, K. Jiménez-García, and I. B. Spielman, Nature (London) **471**, 83 (2011).

[3] M. Aidelsburger, M. Atala, S. Nascimbène, S. Trotzky, Y.-A. Chen, and I. Bloch, Phys. Rev. Lett. **107**, 255301 (2011); P. Hauke *et al.*, *ibid.* **109**, 145301 (2012).

[4] L. J. LeBlanc, K. Jiménez-García, R. A. Williams, M. C. Beeler, A. R. Perry, W. D. Phillips, and I. B. Spielman, Proc. Natl. Acad. Sci. USA **109**, 10811 (2012).

[5] J.-Y. Zhang, S.-C. Ji, Z. Chen, L. Zhang, Z.-D. Du, B. Yan, G.-S. Pan, B. Zhao, Y.-J. Deng, H. Zhai, S. Chen, and J.-W. Pan, Phys. Rev. Lett. **109**, 115301 (2012).

[6] P. Wang, Z.-Q. Yu, Z. Fu, J. Miao, L. Huang, S. Chai, H. Zhai, and J. Zhang, Phys. Rev. Lett. **109**, 095301 (2012); L. W. Cheuk, A. T. Sommer, Z. Hadzibabic, T. Yefsah, W. S. Bakr, and M. W. Zwierlein, *ibid.* **109**, 095302 (2012).

[7] J. Dalibard, F. Gerbier, G. Juzeliūnas, and P. Öhberg, Rev. Mod. Phys. **83**, 1523 (2010).

[8] X.-J. Liu, M. F. Borunda, X. Liu, and J. Sinova, Phys. Rev. Lett. **102**, 046402 (2009).

[9] T. D. Stanescu, B. Anderson, and V. Galitski, Phys. Rev. A **78**, 023616 (2008); C. Wang, C. Gao, C.-M. Jian, and H. Zhai, Phys. Rev. Lett. **105**, 160403 (2010); C.-J. Wu, I. Mondragon-Shem, and X.-F. Zhou, Chin. Phys. Lett. **28**, 097102 (2011).

[10] S. Sinha, R. Nath, and L. Santos, Phys. Rev. Lett. **107**, 270401 (2011); H. Hu, B. Ramachandhran, H. Pu, and X.-J. Liu, *ibid.* **108**, 010402 (2012).

[11] T.-L. Ho and S. Zhang, Phys. Rev. Lett. **107**, 150403 (2011).

[12] Y. Li, L. P. Pitaevskii, and S. Stringari, Phys. Rev. Lett. **108**, 225301 (2012).

[13] T. Ozawa and G. Baym, Phys. Rev. A **85**, 013612 (2012); Phys. Rev. Lett. **109**, 025301 (2012).

[14] J. P. Vyasanakere and V. B. Shenoy, Phys. Rev. B **83**, 094515 (2011); J. P. Vyasanakere, S. Zhang, and V. B. Shenoy, *ibid.* **84**, 014512 (2011).

[15] M. Gong, S. Tewari, and C. Zhang, Phys. Rev. Lett. **107**, 195303 (2011); H. Hu, L. Jiang, X.-J. Liu, and H. Pu, *ibid.* **107**, 195304 (2011); Z.-Q. Yu and H. Zhai, *ibid.* **107**, 195305 (2011).

[16] E. van der Bijl and R. A. Duine, Phys. Rev. Lett. **107**, 195302 (2011).

[17] Y. Zhang, L. Mao, and C. Zhang, Phys. Rev. Lett. **108**, 035302 (2012); Y. Zhang, G. Chen, and C. Zhang, arXiv:1111.4778.

[18] B. Ramachandhran, B. Opanchuk, X.-J. Liu, H. Pu, P. D. Drummond, and H. Hu, Phys. Rev. A **85**, 023606 (2012).

[19] Z. Chen and H. Zhai, Phys. Rev. A **86**, 041604(R) (2012).

[20] Y. Li, G. I. Martone, and S. Stringari, Europhys. Lett. **99**, 56008 (2012).

[21] W. Zheng and Z. Li, Phys. Rev. A **85**, 053607 (2012).

[22] J. Stenger, S. Inouye, A. P. Chikkatur, D. M. Stamper-Kurn, D. E. Pritchard, and W. Ketterle, Phys. Rev. Lett. **82**, 4569 (1999); D. M. Stamper-Kurn, A. P. Chikkatur, A. Görlitz, S. Inouye, S. Gupta, D. E. Pritchard, and W. Ketterle, *ibid.* **83**, 2876 (1999); J. Steinhauer, R. Ozeri, N. Katz, and N. Davidson, *ibid.* **88**, 120407 (2002).

[23] Y. A. Bychkov and E. I. Rashba, J. Phys. C **17**, 6039 (1984).

[24] G. Dresselhaus, Phys. Rev. **100**, 580 (1955).

[25] For the spin-asymmetric case where $g_{\uparrow\uparrow} \neq g_{\downarrow\downarrow}$, one can define the interaction parameters as $G_1 = n(g_{\uparrow\uparrow} + g_{\downarrow\downarrow} + 2g_{\uparrow\downarrow})/8$, $G_2 = n(g_{\uparrow\uparrow} + g_{\downarrow\downarrow} - 2g_{\uparrow\downarrow})/8$, and $G_3 = n(g_{\uparrow\uparrow} - g_{\downarrow\downarrow})/4$. By tuning the parameter δ, the asymmetric effect caused by G_3 can be compensated. The ground state then remains the same as in the spin-symmetric case [12].

[26] Notice that result (8) for $\langle \sigma_x \rangle$ holds in the spin-rotated frame where the Hamiltonian takes the form (4). Since the operators σ_x and σ_z do not commute, the average value of σ_x evaluated in spin space, calculated in the original frame, exhibits an additional oscillatory behavior $\langle \sigma_x \rangle \cos(2k_0 x - \Delta\omega_L t) - \langle \sigma_y \rangle \sin(2k_0 x - \Delta\omega_L t)$, with $\langle \sigma_x \rangle$ and $\langle \sigma_y \rangle$ given by (8) and (9), characterizing the laser potential of Eq. (1) (an analogous result holds for the average value of σ_y).

[27] L. P. Pitaevskii and S. Stringari, *Bose-Einstein Condensation* (Oxford University Press, New York, 2003).

[28] When one approaches the II-III phase transition, most of the contribution to the f-sum rule, in the small q limit, comes from the upper branch of the excitation spectrum.

[29] L. Pitaevskii and S. Stringari, J. Low Temp. Phys. **85**, 377 (1991); Phys. Rev. B **47**, 10915 (1993).

[30] R. M. Wilson, C. Ticknor, J. L. Bohn, and E. Timmermans, Phys. Rev. A **86**, 033606 (2012); L. Santos, G. V. Shlyapnikov, and M. Lewenstein, Phys. Rev. Lett. **90**, 250403 (2003).

[31] At finite temperature T one instead expects the static structure factor to be significantly peaked near the roton minimum, provided the roton energy is small compared to T, as a consequence of the thermal excitations of rotons, similar to what is predicted for quasi-two-dimensional dipolar gases [36].

[32] The symmetry of the static structure factor for exchange of **q** into $-$**q** is a general feature following from the completeness relation and the commutation relation involving the density operators: $S(\mathbf{q}) - S(-\mathbf{q}) = \langle [\rho_{\mathbf{q}}, \rho_{-\mathbf{q}}] \rangle = 0$.

[33] The equation for the spin density takes the form $\partial s / \partial t = k_0 \nabla_x n - \nabla \cdot [s \nabla(\varphi_\uparrow + \varphi_\downarrow) + n \nabla(\varphi_\uparrow - \varphi_\downarrow)]/2 - \Omega \sqrt{n^2 - s^2} \sin(\varphi_\uparrow - \varphi_\downarrow)$, showing that the difference $(\varphi_\uparrow - \varphi_\downarrow)$ between the two phases should be small if the frequency of the oscillation is much smaller than the Raman coupling Ω. The oscillation of the relative phase plays a crucial role in the excitation of the upper branch, whose frequency is of the order of Ω.

[34] S. Hoinka, M. Lingham, M. Delehaye, and C. J. Vale, Phys. Rev. Lett. **109**, 050403 (2012).

[35] S. Stringari, Phys. Rev. Lett. **77**, 2360 (1996).

[36] M. Klawunn, A. Recati, L. P. Pitaevskii, and S. Stringari, Phys. Rev. A **84**, 033612 (2011).